AIAA JOURNAL
Vol. 38, No. 2, February 2000

Technical Notes

TECHNICAL NOTES are short manuscripts describing new developments or important results of a preliminary nature. These Notes cannot exceed 6 manuscript pages and 3 figures; a page of text may be substituted for a figure and vice versa. After informal review by the editors, they may be published within a few months of the date of receipt. Style requirements are the same as for regular contributions (see inside back cover).

Application of Lighthill's Equation to a Mach 1.92 Turbulent Jet

T. Colonius*
California Institute of Technology, Pasadena, California 91125
and
J. B. Freund†
University of California, Los Angeles, Los Angeles, California 90095

Introduction

IT has often been suggested that simulations of turbulent jets could provide the necessary sound source information for jet noise predictions via Lighthill's acoustic analogy.[1] Such an application of Lighthill's equation is useful for two reasons. First, it provides a framework for identifying and modeling acoustic sources in a turbulent flow. Second, it may provide a less expensive means of computing the sound generated by turbulent flows because the flow equations would need to be computed only in the source region.

An important precursor to making such predictions in the general case is to quantify the accuracy of the acoustic field that can be expected for specific flows, given the discrete numerical representation of the source terms. The accuracy depends, on one hand, to what extent computational errors may affect the acoustic sources and, on the other hand, how reliable the approximations are that are made in separating source terms from propagation terms in the acoustic analogy. These issues were addressed in detail for vortex pairing in a two-dimensional mixing layer by Colonius et al.,[2] and the Lighthill acoustic analogy has been successfully applied to an axisymmetric jet[3] and a periodic region of turbulence,[4] but it is as yet unclear to what extent the conclusions of these previous studies apply to a turbulent jet.

A commonly voiced concern is that quadrupole cancellations of the source might be upset by discretization errors, leading to an erroneously more efficient dipole- or monopole-type source (see, for example, the discussion by Crighton[5]). Truncation of the source at a finite location downstream can also lead to enhanced radiation by similarly disrupting cancellations that should occur.[3] In this Note, we address the accuracy of the acoustic analogy prediction given sources determined by a direct numerical simulation of a Mach 1.92 turbulent jet.[6] The results will be compared with the jet noise field computed in that simulation. Details of the computed flowfield (mean flow, turbulent statistics, etc.) and the numerical methodology may be found in Ref. 6 and references therein. Although the simulated jet could not be compared explicitly to an experiment at the same flow conditions, it was shown to have peak noise intensity within a 1–2 dB of jets at comparable Mach numbers. Turbulent stresses and mean flow development were shown to be similarly realistic.[6]

Received 29 May 1999; revision received 15 September 1999; accepted for publication 17 September 1999.

*Assistant Professor of Mechanical Engineering. Member AIAA.
†Assistant Professor of Mechanical and Aerospace Engineering. Member AIAA.

Methodology and Results

We start with the well-known equation of Lighthill[1]:

$$\frac{\partial^2 \rho}{\partial t^2} - a_o^2 \frac{\partial^2 \rho}{\partial x_j \partial x_j} = \frac{\partial^2 T_{ij}}{\partial x_i \partial x_j} \tag{1}$$

where

$$T_{ij} = \rho u_i u_j + (p - a_o^2 \rho)\delta_{ij} \tag{2}$$

and the viscous stresses have been neglected. We use the full instantaneous flowfield, including the density, to compute the Lighthill source given by the right-hand side of Eq. (2). The instantaneous flowfield from simulation was archived at roughly 7000 times (at increments of 10 computational time steps) after a statistically stationary state was achieved. For practical reasons, the data were saved only at every other computational node. A large number of terms are involved in computing Lighthill's source in cylindrical coordinates (the transformations are straightforward but tedious and will not be reproduced here), including second spatial derivatives of the computational data and some terms with $\mathcal{O}(1/r^2)$ coordinate singularities. To remedy obvious numerical difficulties near $r = 0$, the instantaneous flow data were interpolated onto a Cartesian mesh in this region, and the right-hand side of Lighthill's equation was then computed in Cartesian coordinates. It appeared that the coarser mesh and the complexity of the Lighthill source term accentuated the standard problems associated with this coordinate singularity. Sixth-order compact schemes[7] were used for differentiation of the data, and fourth-order B-splines were used for the interpolation.

In Fig. 1 the instantaneous acoustic field (dilatation) from the simulation is plotted for the axisymmetric and first azimuthal modes ($m = 0$ and 1, respectively). These two azimuthal modes account for approximately 80% of the noise radiation from this jet. The acoustic field is clearly dominated by Mach waves at angles between 45 and 55 deg from the jet axis, and the apparent source of these waves is a region of the jet between about $x = 10r_o$ and $20r_o$. This corresponds

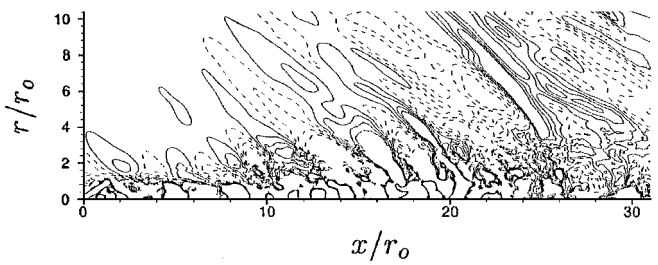

Azimuthal mode $m = 0$; eight contours between -0.01 and 0.01

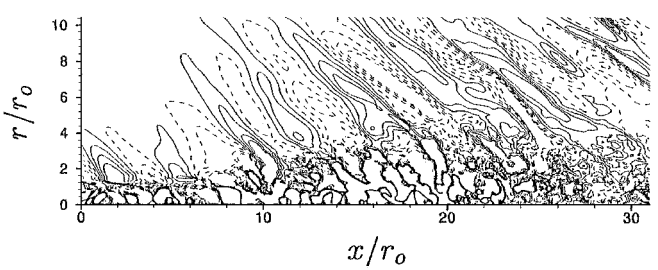

Azimuthal mode $m = 1$; eight contours between -0.005 and 0.005

Fig. 1 Contours of $r_o \nabla \cdot \boldsymbol{u}/U_j$ in the acoustic field (negative contours are dashes).

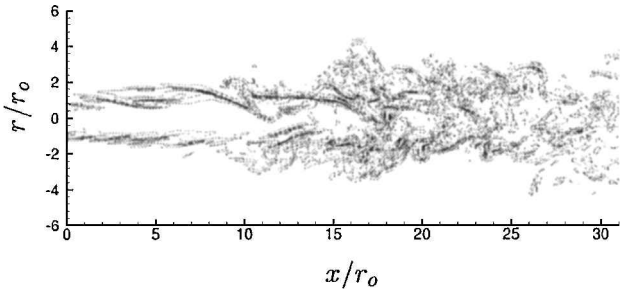

Fig. 2 Contours of the instantaneous $T_{ij,ij}$ in the plane $\theta = 0, \pi$: 10 evenly spaced contours between $\pm 5\rho_j U_j^2/r_o^2$.

to the region where the potential core closes and where it might be expected that large-scale structures propagate with speeds supersonic relative to the ambient.

Figure 2 shows an instantaneous visualization of the Lighthill source term $T_{ij,ij}$ at the plane $\theta = 0, \pi$ through the jet axis at the same instant in time as the acoustic fields plotted in Fig. 1. It is clear that, instantaneously, the smallest scales are dominant contributors to the total source. Although this may at first seem inconsistent with the view of the wave fields of Fig. 1, it is important to recall that only Fourier components with supersonic phase velocities radiate to the far field. The acoustic efficiency of the sources is also likely related to their size, with larger scales potentially making greater contributions.

To determine the acoustic field from the computed source, Eq. (1) must be solved. A variety of methods are available for this task. From an analytical point of view, the simplest method would be to invert the wave operator with the appropriate Green's function. However, the resulting integrals depend on the source at retarded times. Given the large amount of data that would have to be sorted and interpolated for every such combination of source and observer location, this approach was deemed impractical. Instead we employed the less computationally intensive method (at least for computing the sound out to moderate distances from the jet) of solving the wave equation directly in the time domain using finite differences. The wave equation was discretized in x and r with the same sixth-order-accurate compact finite difference scheme used in the jet computations and integrated forward in time with a fourth-order Runge–Kutta time algorithm. The source was Fourier transformed in the azimuthal direction because the wave equation is linear and each azimuthal mode may, in turn, be found independently. The computational grid was chosen to be identical to that on which the source data were saved except that in the radial direction we interpolated the source (using a sixth-order-accurate compact interpolation scheme) to a staggered mesh to facilitate differencing through the polar coordinate singularity.[8] One-dimensional characteristic boundary conditions were used together with a buffer region near the computational boundary, where the damping terms were added to the wave equation to attenuate reflections from the boundaries.[9]

The source terms at a given instant in time were computed by cubic spline interpolation of the sources at the discrete intervals in time available from the flow simulation. To avoid sharp initial transients produced by activating the source discontinuously at $t = 0$, the source was ramped-up over a time period that was long compared to the dominant frequencies in the acoustic field.

In addition, the computed source was spatially windowed with a function that smoothly decayed from unity to zero for $x/r_0 < 3$, $x/r_0 > 32$, and $r/r_0 > 3$. The window transition was accomplished with a hyperbolic tangent function over a width of r_0. This rather aggressive windowing of the sources should be contrasted to the methods employed in previous studies of unsteady laminar flows,[2,3] where the detailed nature of the source terms in frequency space had to be known a priori to achieve an accurate truncation.

In Fig. 3 the acoustic field found by the method outlined is compared with the simulation solution for the axisymmetric and first azimuthal modes, respectively. The dilatation is plotted along lines of constant r in the acoustic field. The quantitative agreement between the Lighthill predictions and the flow simulation is quite good, especially for the first azimuthal mode.

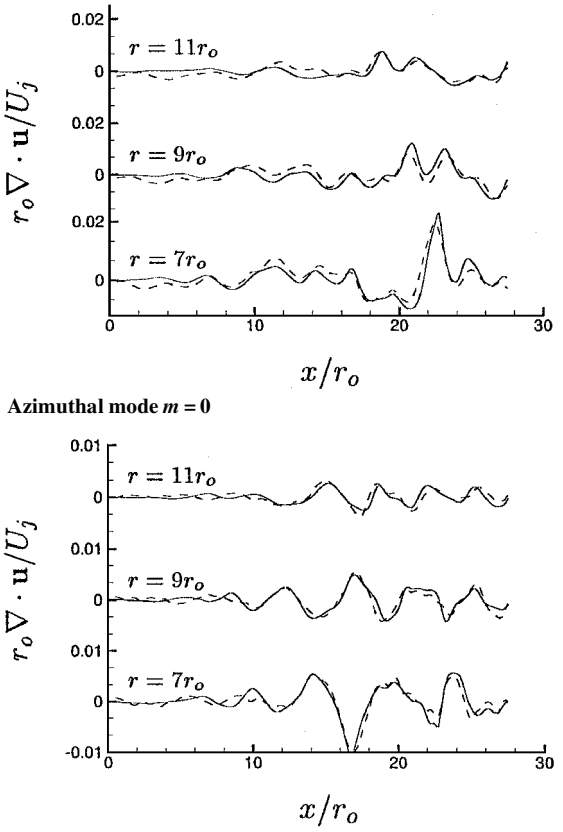

Fig. 3 Comparison of the instantaneous dilatation from the simulation data (——) and solution of Lighthill's equation (- - - -).

Note that the good agreement between the flow simulation and Lighthill's equation is obtained despite the aggressive source windowing discussed. Apparently in the turbulent jet there is sufficient decay or decorrelation of the sources by $x/r_0 = 32$ to obviate the need for a more careful truncation procedure. The agreement also confirms the very minor impact that viscous terms would have on the radiated sound.

The Lighthill solution was found to be somewhat contaminated by apparently erroneous high-wave-number sound, and some spurious smooth waves were also evident. (These can be seen as smooth oscillations for small x in the curves of Fig. 3.) We suspect that the high-wave-number noise is primarily due to differentiation of the computational data on the coarser mesh on which the flow was simulated. Another similar possibility is that aliasing caused by saving the data at every other mesh point without first filtering the solutions on the finer mesh spawned some spurious high-wave-number sound waves. However, because the physical waves have a much lower wave number than the spurious waves, smoothing of the data (linear filtering) effectively eliminates the spurious noise without significantly affecting the generation of the smooth waves from the computed source.

Conclusions

The acoustic analogy approach was directly verified for a fully turbulent Mach 1.92 jet. Because the full source (save the viscous contributions) was used in computing the acoustic field, this result is, in a limited sense, a consistency check on the numerics. However, it has often been suggested that artifacts of the discretization could lead to more powerful sound sources than the turbulence, which was shown not to be the case in the present calculations. Moreover, it was found that a straightforward truncation of the turbulent sources did not lead to spurious radiation, as had been the case in previous calculations with unsteady laminar flows.

This is an important first step toward analyzing the details of the acoustic sources in the jet. For example, the source may now be confidently decomposed in a variety of ways to isolate contributions

from different scales of motion or from different constituent components of the source, for example, linear vs nonlinear terms. Such analysis will be presented in future studies.

Acknowledgments

The first author acknowledges the support of the National Science Foundation, under Grant CTS-9501349. The work was conducted as part of the 1998 Center for Turbulence Research Summer Program, and the authors gratefully acknowledge many helpful comments from Sanjiva Lele and Parviz Moin.

References

[1]Lighthill, M. J., "On Sound Generated Aerodynamically I. General Theory," *Proceedings of the Royal Society of London, Series A*, Vol. 211, 1952, p. 564.

[2]Colonius, T., Lele, S. K., and Moin, P., "Sound Generation in a Mixing Layer," *Journal of Fluid Mechanics*, Vol. 330, 1997, p. 375.

[3]Mitchell, B., Lele, S., and Moin, P., "Direct Computation of the Sound Generated by Vortex Pairing in an Axisymmetric Jet," *Journal of Fluid Mechanics*, Vol. 383, 1999, p. 113.

[4]Whitmire, J., and Sarkar, S., "Validation of Acoustic Analogy Predictions for Sound Radiated Turbulence," *Physics of Fluids* (to be published).

[5]Crighton, D. G., "Computational Aeroacoustics for Low Mach Number Flows," *Computational Aeroacoustics*, edited by J. C. Hardin and M. Y. Hussaini, Springer–Verlag, New York, 1993, pp. 50–68.

[6]Freund, J. B., Lele, S. K., and Moin, P., "Direct Simulation of a Mach 1.92 Jet and Its Sound Field," AIAA Paper 98-2291, 1998; also *AIAA Journal* (submitted for publication).

[7]Lele, S. K., "Compact Finite Difference Schemes with Spectral-Like Resolution," *Journal of Computational Physics*, Vol. 103, No. 1, 1992, p. 16.

[8]Mohseni, K., and Colonius, T., "Numerical Treatment of Polar Coordinate Singularities," *Journal of Computational Physics* (to be published).

[9]Freund, J. B., "Proposed Inflow/Outflow Boundary Condition for Direct Computation of Aerodynamic Sound," *AIAA Journal*, Vol. 35, No. 4, 1997, pp. 740–742.

M. Samimy
Associate Editor

Numerical Optimization of the Suction Distribution for Laminar Flow Control

O. R. Tutty,* P. Hackenberg,† and P. A. Nelson‡
University of Southampton, Southampton, England SO17 1BJ, United Kingdom

Introduction

THE possibility of controlling boundary layers to delay transition is a subject that has received much attention within the aerodynamics research community because of the lower skin-friction drag in laminar flow. It has long been known that small amounts of surface suction can, in theory, greatly enhance the stability characteristics of an attached boundary layer and thereby reduce drag and, hence, operating costs by delaying transition. At Southampton over the past eight years there has been a program of research into the experimental application of distributed suction for the automatic control of boundary-layer transition. In the initial work a plate with two independent suction panels was used, either with or without a freestream pressure gradient. The individual suction flow rates were controlled, maintaining transition at a desired location while minimizing a cost function based on the sum of squares of the suction flow rates,[1,2] which gives a rough approximation to the power consumption of the pumps used in the suction system. This formulation, which is based on the design requirements for a nacelle, gives a nonlinearly constrained optimization problem. To solve it, an algorithm was developed[3] based on a gradient projection method.

In addition to the experimental work, which is detailed in Refs. 1–3, a complementary program of theoretical modeling has been performed. This work was aimed at both modeling the experiments and extending the scope of the research by considering more suction panels and more realistic geometries such as NACA airfoils. The modeling consists of the numerical solution of an interactive boundary-layer formulation for the flow, a linear stability analysis using the Orr–Sommerfeld equation, and transition prediction using the e^N method, followed by an update of the suction flow rates using the same basic strategy as that used in the experiments. As formulated, it mimics the experiments, which enables us to investigate more complex configurations. This Note presents some of the results from the theoretical modeling. Further details of our recent work in this area can be found in Ref. 4.

The calculations described were performed for air at standard conditions ($\nu = 1.5 \times 10^{-5}$ m^{2}s^{-1}) with a freestream velocity of $\tilde{U} = 20$ ms^{-1}, a reference length of $\tilde{L} = 1$ m, and a value of $N_T = 4.3$ in the e^N method, corresponding to a freestream turbulence level of approximately 0.5% as found in the wind tunnel used for the experiments.

Flat Plate Configuration

With no suction, transition is predicted to occur at $x \approx 0.93$, so that any useful suction panel must have at least its leading edge upstream of this position. Calculations were performed using a single suction panel in the region $0.4 \leq x \leq 0.72$. Initially, as suction is applied, the change in x_T is close to linear, with a relatively small amount of suction moving transition a significant distance downstream until $x_t \approx 1.4$, when $C_q = -\bar{v}_w / \tilde{U} \approx 10^{-4}$. However, as more suction is applied, the slope of the curve changes until the transition asymptotes to a constant position between $x = 1.6$ and 1.65. When this occurs, the boundary layer on the suction panel is extremely thin, and increasing the suction flow rate has little effect on the stability characteristics of the flow downstream of the panel. Hence, for a single panel, after a certain point, further suction effort is largely wasted in terms of delaying the onset of transition. Furthermore, a reasonable estimate of the maximum distance that transition can be moved downstream is obtained by adding the transition position with zero suction to the position of the downstream end of the suction panel ($x_T = 0.93 + 0.72 = 1.65$).

A two-panel configuration, similar to that used in the experiments, was also investigated. The panels were at $0.28 \leq x \leq 0.48$ and $0.58 \leq x \leq 0.78$. Contours of the value of x_T for combinations of the suction flow rates are shown in Fig. 1, as is the contour of the cost function for the optimum value when $x_d = 1.5$. In this case, it is clear that there is a single global optimum for each value of x_d and that for low values of x_d the optimum has essentially the same suction flow rate on both panels. The latter result was also found in the experiments.[2] The transition position and suction flow rates plotted against the iteration number k are shown in Fig. 2. There

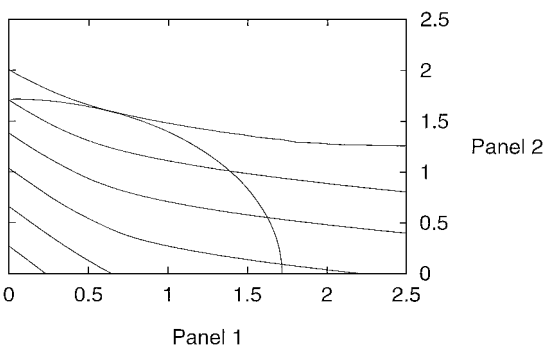

Fig. 1 Transition position for two suction panels as a function of the $C_q \times 10^4$; contours are for constant x_T up to $x_T = 1.5$ in increments of 0.1; also shown is the contour for the optimum value of the cost function when $x_d = 1.5$. The optimum is given by the point closest to the origin where the lines are tangential.

Received 8 October 1998; revision received 25 August 1999; accepted for publication 1 September 1999.

*Reader, School of Engineering Sciences.
†Professor, Institute of Sound and Vibration Research.
‡Research Assistant, Institute of Sound and Vibration Research.